Assembly of the Tetra-Mn Site of Photosynthetic Water Oxidation by Photoactivation: Mn Stoichiometry and Detection of a New Intermediate†

Gennady M. Ananyev and G. Charles Dismukes*

Hoyt Laboratory, Department of Chemistry, Princeton University, Princeton, New Jersey 08544

Received November 8, 1995; Revised Manuscript Received February 2, 1996⊗

ABSTRACT: The process of photoactivation, the assembly of the water-oxidizing complex (WOC) of photosystem II (PSII) membranes, has been examined using two major improvements in methodology. First, a new lipophilic chelator, *N,N,N′,N′*-tetrapropionato-1,3-bis(aminomethyl)benzene (TPDBA), has been used that permits complete extraction of both manganese and calcium and the three extrinsic WOC polypeptides while minimizing damage to the apo-PSII protein and, importantly, eliminating the need to use reductants. Second, an ultrasensitive, fast-response, polarographic cell and detection system were built. The apparatus features (a) an ultrabright red light-emitted diode (LED) for controlling the light intensity, pulse duration, and dark intervals, features critical for minimization of photoinhibition; (b) a microvolume (5 μL) O_2 polarographic cell (Clark type) fitted with a thin silicone membrane for rapid response (100 ms); and (c) DC/AC preamplifier integrated into the microcell and interfaced to a band-pass AC amplifier. The sensitivity enables detection of $\sim 5 \times 10^{-14}$ mol of O_2 per flash at a signal to noise = 5/1. These improvements permit 100-fold lower Mn concentrations to be explored. Under optimum conditions, complete recovery of O_2-evolving activity could be restored compared to that of PSII membranes depleted of the three extrinsic polypeptides (35% V_{max} *vs* intact PSII). Titration of the photoactivation steady-state O_2 yield, Y_{ss}, and the half-time for recovery, $t_{1/2}$, *vs* Mn concentration demonstrate that 4.0 Mn/P680 are cooperatively taken up at 95% restoration of Y_{ss} and that 1.1−1.2 Mn atoms are involved in the rate-limiting photolytic step under steady-state conditions. Due to minimization of photoihibition, this intermediate exhibits a single exponential recovery kinetic over the entire population of PSII centers. Mn atoms in excess of 4 Mn/P680 accelerate the rate of photoactivation but decrease the yield above 8−10 Mn/P680. Maxima in both Y_{ss} and $t_{1/2}$ are observed at similar electrochemical potentials of the medium, 380 and 340 mV, respectively. We attribute this maximum to either elimination of a recombination reaction between the redox-active tyrosine-161 of the D1 polypeptide (Y_Z^+) and an electron acceptor, possibly cytochrome b_{559}, or stabilization of an intermediate in photoactivation. At low Mn^{2+} concentrations, a new pre-steady-state kinetic intermediate which binds fewer than 4 Mn atoms can be directly observed. This early kinetic phase has a rate that depends on Mn concentration and is independent of the electron acceptor identity and concentration.

Photoactivation, the *in vivo* process by which the essential inorganic cofactors (manganese, calcium, and chloride) bind to the apo-PSII[1] core complex and under illumination form a functional O_2-evolving enzyme, is an example of protein-templated assembly of a reactive catalytic cluster (Cheniae & Martin, 1971; Radmer & Cheniae, 1971, 1977). The cluster is unstable in solution and has not been "extruded" from the protein as an intact core, unlike the stable inorganic cores of iron−sulfur proteins and the Mo−Fe cofactor of nitrogenase. The mechanism of photoactivation is a fundamental problem in bioinorganic chemistry, being common to all oxygenic photosynthetic organisms.

In the past 25 years, many studies have provided insight into the photoactivation process, including (1) the role of inorganic cofactors (Mn^{2+}, Ca^{2+}, and Cl^-) and experimental conditions, such as light intensity, pH, type of buffer and exogenous electron acceptor, and the method for removal of Mn (Ono & Inoue, 1983a,b; Yamashita & Ashizawa, 1983; Hsu et al., 1987; Ananyev et al., 1988b; Miller & Brudvig, 1989, 1990; Miyao-Tokutomi et al., 1990; Miyao & Inoue, 1991; Tamura et al., 1991, 1992); (2) identification of essential amino acid residues for assembly and possible Mn ligands (Tamura et al., 1989a, 1992; Preston & Seibert, 1989, 1991); (3) The time course for recovery of O_2 evolution under continuous and intermittent light leading to a kinetic model for assembly of the cluster, involving sequential light and dark steps of Mn ligation and photooxidation leading to formation of the tetra-Mn cluster (Tamura & Cheniae, 1987a,b); and (4) a model for reassembly of the extrinsic polypeptides of PSII and their role in enhancing the affinity

† This work was supported by the National Institutes of Health (Grant GM39932).

* To whom correspondence should be addressed. Fax: (609) 258-1980. E-mail: dismukes@chemvax.princeton.edu.

⊗ Abstract published in *Advance ACS Abstracts,* March 1, 1996.

[1] Abbreviations: Chl, chlorophyll; DCBQ, dichlorobenzoquinone; DCIP, 2,6-dichlorophenolindophenol; LED, light-emitted diode; MES, 2-(*N*-morpholino)ethanesulfonic acid; P680, primary electron donor; PSII, photosystem II; Pheo, primary pheophytine electron acceptor of PSII; Q_A and Q_B, primary and secondary plastoquinone electron acceptors; RC, reaction center; $t_{1/2}$, half-time kinetics of assembly of the tetra-Mn cluster; TEMED, *N,N,N′,N′*-tetramethylethylenediamine; THED, *N,N,N′,N′*-tetrakis(2-hydroxypropyl)ethylenediamine; TMDM, *N,N,N′,N′*-tetramethyldiaminomethane; TMG, tetramethylguanidine; TPDBA, *N,N,N′,N′*-tetrapropionato-1,3-bis(aminomethyl)benzene; V_{O2}, maximal rate of O_2 evolution at saturated continuous light after pulse light activation; Y_{ss}, steady-state level kinetics of pulse light photoactivation of O_2 evolution; Y_Z^+, redox-active tyrosine-161 of the D1 polypeptide; WOC, water-oxidizing complex; S/N, signal to noise.

0006-2960/96/0435-4102$12.00/0

or stability of one or more of the inorganic cofactors (Ono & Inoue, 1983a; Tamura et al., 1989b; Ebina & Yamashita, 1992; Blubaugh & Cheniae, 1992).

Model systems for studying *in vitro* photoactivation have included isolated chloroplasts and PSII membranes after extraction of manganese, calcium, and extrinsic polypeptides and chloroplasts isolated from greening plants grown under intermittent flashing illumination (Ono & Inoue, 1983a). The methods used for complete extraction of cofactors have relied on using reductants such as NH_2OH, NH_2NH_2, $DCIPH_2$, or hydroquinone (Yamashita & Tomita, 1974; Radmer & Cheniae, 1977; Miyao & Inoue, 1991), usually accompanied by washing in alkaline buffer (0.8−1 M Tris-HCl buffer). Reductants like NH_2OH facilitate removal of Mn from the WOC by prereduction to the labile Mn^{2+} valence state. However, residual NH_2OH that is not removed prior to photoactivation poses a potential problem in slowing the kinetics of photoactivation, as also does the use of divalent cations. Using NH_2OH and Tris free base to extract PSII membranes, Tamura and Cheniae (1987a,b) found that 90% Mn could be released and that only light and Mn^{2+} were essential for Mn religation to the apo-PSII but that Ca^{2+} addition was required for maximal expression of water oxidation activity by the photoligated Mn. More recently, Chen et al. (1995) have shown that Ca^{2+} is also needed for prevention of ligation and photooxidation of nonfunctional Mn in high valency states that inhibits activity. Divalent cations like Mg^{2+} and Ca^{2+} appear to compete with Mn^{2+} for nonspecific binding sites (Miller & Brudvig, 1989).

Complete removal of Mn (>97%) and the extrinsic water-soluble proteins (17, 24, and 33 kDa) from PSII membrane fragments has also been achieved by incubation with 1 M Tris/0.5 M $MgCl_2$ (pH 7.8), while O_2-evolving activity can be restored to 50% with Mn^{2+}, Ca^{2+}, and Cl^- (Klimov et al., 1986, 1987; Shafiev et al., 1988). This method benefits from the absence of reductants but employs divalent ions and mildly denaturating conditions.

The use of intact chloroplasts and thylakoid membranes poses the additional problem of restricted accessibility of the soluble cofactors to the membrane-associated PSII centers. The more highly resolved O_2-evolving core complexes (40−60 Chl/P680) have the disadvantage of damage to the electron acceptor side, leading to enhanced rates of photoinhibition in the absence of Mn [for review see Debus (1992)]. Triton X-100-extracted PSII membranes (200−250 Chl/P680) comprised of exposed or disrupted grana membranes appear to be the best compromise between adequate accessibility which appears not to limit the photoactivation kinetics and the retaining of low levels of photoinhibition in the absence of Mn.

The choice of electron acceptor is also critical, as it must interact rapidly with the endogenous acceptor in the oxidized form, while not reacting with the exposed WOC in either the reduced or oxidized form. The quinone acceptors, ferricyanide, and DCIP have all been examined. It has been reported that 5−20 μM DCIP is optimal for photoactivation with 1 mM Mn^{2+} (Miyao & Inoue, 1991) or 0.8 mM K_3FeCN_6 with 4−8 μM Mn^{2+} (Ananyev et al., 1988a,b; Shafiev et al., 1988).

The number of Mn^{2+} ions needed for photoactivation has been estimated in previous studies by measurement of the number of Mn ions which bind to the apo-PSII protein. These results show a range of stoichiometries from 2 to 6 Mn atoms/RC of PSII [for reviews see Cheniae (1980), Brudvig et al. (1989), Debus (1992), and Callahan and Cheniae (1985), Dismukes (1986), Dismukes et al. (1982), Pauly and Witt (1992)]. These earlier methods have all required a large excess of Mn relative to P680, typically 100-fold, in order to observe a maximal yield of photoactivation and to minimize photoinhibition. Photoinhibition of apo-PSII is a severe problem at low Mn concentrations and at continuous white light (Blubaugh & Cheniae, 1990; Chen et al., 1992).

Examination of the early intermediates in photoactivation has been hampered by the insensitivity of the commercial Clark-type electrode used to assay O_2 concentration. To achieve measureable O_2 concentrations during photoactivation with commercial Clark-type cells, one needs to use sample volumes on the order of 1 mL or larger and high concentrations of the inorganic cofactors, typically 100-fold in excess of the PSII concentration in order to suppress photoinhibition. This limitation has made it impossible to use stoichiometric concentrations of the inorganic cofactors as a means of probing the existence and structure of early intermediates formed during photoactivation prior to the rate-limiting step.

We have overcome some of these limitations by developing an integrated Clark-type electrode and illumination cell capable of high sensitivity, fast response time, versatile control of the light and dark periods, and virtual elimination of photoinhibition by wavelength and intensity selection using LED illumination. Another key advance is the development of a new chelator for extraction of Mn and Ca which optimizes the photoactivation yield. We use these new tools to kinetically resolve the first light-induced intermediate in the photoactivation process and to reexamine in more detail the stoichiometry of Mn atoms required for assembly of the tetra-Mn cluster WOC.

MATERIALS AND METHODS

PSII-enriched membrane fragments were prepared from market spinach using the method of Berthold et al. (1981) with some minor modifications (Ghanotakis et al., 1984). The samples (1 mg of Chl/mL) were frozen with 10% glycerol in liquid nitrogen and stored at −196 °C until they were slowly thawed and washed once in a medium containing 300 mM sucrose, 35 mM NaCl, and 25 mM MES/NaOH buffer (pH 6.0) (assay medium). The oxygen evolution rate under continuous illumination (V_{O2}) of the untreated PSII membrane fragments with 0.8 mM K_3FeCN_6/1.2 mM DCBQ as electron acceptors was 400−500 μmol of O_2/(mg of Chl·h). The concentration of the RC PSII was measured from the photoinduced absorption changes of Pheo at 685 nm with the extinction coefficient $\epsilon = 0.32 \times 10^5\ M^{-1}\cdot cm^{-1}$ (Klimov et al., 1982).

Manganese and calcium were removed from PSII membranes (0.25−1.0 mg of Chl/mL) using the normal assay medium along with 25−35 mM TPDBA and 1 mM ascorbate. Ascorbate decreases the concentration of TPDBA needed for complete removal of Mn to a few millimolar. It is removed by the washing procedure, and residual ascorbate is oxidized by ferricyanide used in the buffer. Other diamino derivative metal ion chelators were also used instead of TPDBA at the following concentrations: 8−11 mM TMG, 10−15 mM TMDM, 15−20 mM TEMED (Ananyev et al., 1992), or 60−80 mM THED. However, TPDBA provides

both complete removal of calcium and manganese (residual oxygen-evolving activity of apo-PSII is equal to zero) and maximal photoactivation yield in comparison to all of these diamino derivatives. It was necessary to optimize the concentration of chelator individually for each PSII sample to permit complete Mn extraction while the loss of the photoactivation yield was minimized. This concentration depends on the time of storage of the PSII membrane fragments in liquid nitrogen (maximal time, ~1.5 month) and, presumably, the residual detergent concentration. After dark incubation in the chelator medium for 90 s at 20 °C, followed by rapid cooling to 2 °C and an additional 5 min of dark incubation, the PSII suspension was pelleted by centrifugation for 4 min (14 000 rpm in an Eppendorf-type centrifuge 5415). The pellet was washed three times and resuspended in the assay medium at 250 μg of Chl/mL (1 μM RC PSII).

Photoactivation and polarographic detection of O_2 were performed directly in a home-built microcell with 5 μL volume and a 0.3 mm sample thickness. The working electrode was fabricated from an alloy of 75% Pt + 25% Ir, which ensures long term mechanical stability and chemical resistance. The 4 mm diameter electrode surface was polished to a bright reflective finish using a fine diamond abrasive (size of particles, <1 μm) to achieve rapid response and high sensitivity. The working electrode was covered with a dimethylsilicone membrane (type MEM-100, Membrane Product Co., U.S.A., or type FUM membrane, Russia) with a thickness of 1−5 μm. This choice of membrane and thickness in combination with the small sample volume and electrode surface homogeneity allows for a faster response time of 100 ms compared to about 1−3 s for the standard 5 μm Teflon membrane in commercial cells. The O_2 sensitivity is generally a trade-off between membrane permeability and response time.

A high-surface area, low-resistance Ag/AgCl reference electrode was fabricated in the shape of a helix coil from silver wire (0.4 mm in diameter and 40 cm in length) and polarized for 5 min at +600 mV in 0.1 M HCl to create a AgCl layer. The helix surrounded the Pt−Ir working electrode and had an area 40 times greater. The difference current signal between the reference and working electrodes (immersed in 100 mM to 1.0 M KCl) was amplified. A precision low-noise current-to-voltage converter (two operational amplifiers OP 07, Analog Devices, U.S.A.) (Horowitz & Hill, 1993) with an input impedance of <10 Ω, an input current conversion of 1 nA to output voltage 3.25 mV, and a band width from 0 to 1000 Hz was fabricated directly into the microcell to minimize environmental electromagnetic interference. The output signal was further amplified 20−100-fold using a commercial amplifier with adjustable high- and low-frequency filters (model 113 Low-Noise AC-Preamplifier, EG & G Princeton Applied Research Corp., U.S.A.). For the most sensitive measurements, the frequency band width was restricted to the region from 0.3 to 3 Hz. As a measure of sensitivity, the apparatus has a S/N ratio of 5/1 for detection of the O_2 signal produced in untreated PSII membranes at a concentration of 1 μg of Chl/mL (4 nM P680) by exposure to a series of saturating 4 μs xenon flashes. The sensitivity enables detection of $\sim 5 \times 10^{-14}$ mol of O_2 per flash.

For both pulse and continuous illumination, the cell is surrounded by one or four ultrabright LEDs with a wavelength maximum of 660 nm (HLMP-8102, Hewlett-Packard, U.S.A.). In the pulse mode of operation, flashes of 0.1−60 ms duration with intervening dark intervals from 100 ms to 10 s could be achieved. The light intensity was adjustable between 0 and 8 mW/cm^2 (0−20 mA current) and between 8 and 80 mW/cm^2 (20−200 mA) for continuous and pulse light regimes, respectively. Light intensities were measured using a power/energy meter (model 362, Scientech, U.S.A.).

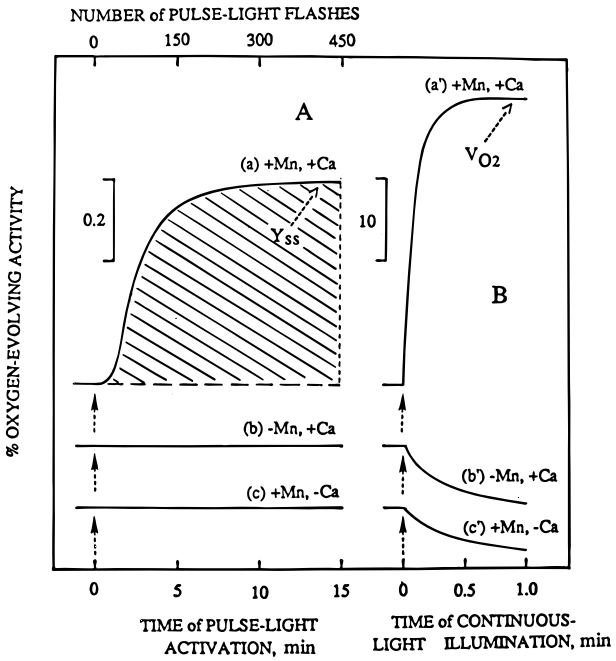

FIGURE 1: (A) Typical kinetics of the rate of recovery O_2 evolution by photoactivation in TPDBA-extracted BBY PSII membranes using light pulses from the LED illumination source: (a) in the presence of 8 μM $MnCl_2$ and 8 mM $CaCl_2$, (b) only 8 mM $CaCl_2$, (c) only 8 μM $MnCl_2$. (B) Traces a′, b′, and c′ were obtained from the samples in panel A (a, b, and c), respectively, by using continuous red light illumination of saturating intensity after photoactivation. Each sample was incubated in the dark for 20 s after photoactivation by the pulse light. The TPDBA-extracted PSII membranes (1 μM P680) were suspended in assay medium [25 mM MES/NaOH (pH 6.0), 35 mM NaCl, 300 mM sucrose, and 0.8 mM K_3FeCN_6] and were dark adapted for 30 min at 20 °C. The photoactivation conditions were as follows: t_{light} = 20 ms, t_{dark} = 2 s, and light intensity I_p = 80 mW/cm^2 and I_c = 8 mW/cm^2 for pulse and continuous light illumination, respectively.

RESULTS

Kinetics of Photoactivation of TPDBA-Extracted PSII Membranes. Figure 1A demostrates the time course for recovery of O_2 evolution in the presence of 8 μM $MnCl_2$ and 8 mM $CaCl_2$ (top) and 8 mM $CaCl_2$ and the absence of Mn (middle) or Ca (bottom). All samples contain 1 μM P680 as PSII membranes and 0.8 mM K_3FeCN_6 as the electron acceptor. Illumination is provided by a series of light pulses (refer to Figure 3); about 300−450 pulses (12−15 min pulse light illumination) are required to reach the maximum yield of recovery of the O_2 evolution rate, symbolized as Y_{ss} in all figures. The individual flashes are not shown in the figure; only the envelope of the signal response is plotted. At Y_{ss}, each flash produces a maximal electrical current approximately 3.8 nA compared to the noise which has an equivalent current of 5−20 pA. Hence, the typical S/N ratio is 200−700. This value is critical for measurement of the O_2 yield at the initial step of photo-

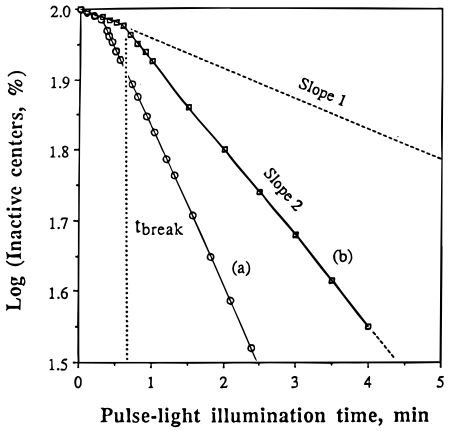

FIGURE 2: Semilogarithmic plot of the percent of inactive centers *vs* integrated pulse light illumination time. Two plots for 40 μM (a) and 8 μM Mn^{2+} (b) are given. The oxygen-evolving activity of untreated PSII membranes was equal to 420 μmol of O_2/(mg of Chl·h) (100%) with 0.8 mM K_3FeCN_6 as the electron acceptor. The assay conditions are the same as those in Figure 1.

activation. Y_{ss} does not decrease after 20−25 min of pulse illumination, indicating insignificant photoinhibition following photoactivation.

Figure 1B (top) shows that pulse light photoactivation of PSII followed by subsequent illumination with continuous red light immediately produces O_2 at a rate 70 times greater than the Y_{ss} level or 30−35% of the untreated control PSII. Thus, Y_{ss} corresponds to 0.2−0.3% of the O_2 rate observed using saturating continuous illumination in an untreated PSII control. The ratio $V_{O2}/Y_{ss} = 60-70$ corresponds closely to the ratio of time periods for t_{dark}/t_{light} durations, as expected assuming that the rate-limiting steps for electron transfer under continuous and pulsed light excitation are the same.

In the absence of Mn^{2+} and/or Ca^{2+}, no photoactivation by pulse light excitation occurs (Figure 1A, traces a and b), and only weak O_2 uptake takes place under continuous illumination (Figure 1B, traces b′ and c′). This result confirms that all functional manganese was removed completely from the reaction medium. The slow O_2 uptake signal is suppressed under pulse light illumination by selection of the low-frequency filter (0.3 Hz). The half-time, $t_{1/2}$, for photoactivation of TBPDA-extracted PSII is equal to 80−150 s, or 2 times faster than that reported for standard NH_2OH-extracted PSII membranes using weak continuous illumination with 1 mM $MnCl_2$, 50 mM $CaCl_2$, and 100 μM DCIP (Tamura & Cheniae, 1987a,b). In our apparatus, the kinetics of photoactivation using 5 mM NH_2OH-extracted PSII membranes that were washed to remove excess NH_2OH also gave longer $t_{1/2}$ by at least 10%. However, the initial level of O_2 evolution present prior to photoactivation was 5−10% *vs* 0% in TPDBA-extracted membranes (data not shown). Elimination of this residual activity could be achieved using higher concentrations of reductant, but with a further increase in $t_{1/2}$ and loss in Y_{ss}.

Figure 2 shows a semilogarithmic plot of the percent of the inactive (but photoactivable) apo-PSII centers *vs* total time of pulse light illumination. Like Tamura and Cheniae (1987b), we assumed that the maximum photoactivation was equivalent to complete conversion of the inactive apo-S-state complex to the active S-state complex. We also assume that at the initial moment of photoactivation all centers are inactive. The sharp break in the curve shows that recovery of O_2 evolution is a biphasic process, with either two sequential kinetic phases of different rates or two populations of PSII centers having different rates. The slow initial phase is seen only at limiting concentrations of added Mn and only if the apo-PSII membranes have been completely depleted of Mn from the WOC prior to photoactivation. It is essential that the residual O_2-evolving activity of the apo-PSII membranes be less than 0.1−0.5% in order to reproducibly observe the initial kinetic phase (slope 1). For this reason, reductant-treated apo-PSII membranes are unsatisfactory for observation of this initial phase. Figure 2 also shows that addition of 5 times more Mn^{2+} (40 μM) shifts the time where the break between slope 1 and slope 2 occurs from 35−40 s (at 8 μM Mn^{2+}) to 10−12 s (at 40 μM Mn^{2+}).

Dependence of Photoactivation on Light and Dark Pulse Times. Figure 3A illustrates the dependence of the final V_{O2} observed after photoactivation is completed on the light pulse duration used for photoactivation obtained at a fixed dark interval of 2 s. Figure 3B gives the dependence of V_{O2} on the dark interval at a fixed light pulse duration of 40 ms. In the both cases, O_2 evolution under continuous illumination is measured after pulse light photoactivation is complete and Y_{ss} is attained. Figure 3A demonstrates that a rate of delivery of photons either too rapidly or too slowly decreases Y_{ss}, producing an optimum flash period of about 30−60 ms. At flash durations shorter than 30 ms, there is a rapid drop in photoactivation. This phase corresponds to a kinetic step which requires a half-time of about 8−10 ms in order for the next photon to be processed and advance toward photoactivation. The descending phase above pulse durations of 60 ms reveals a competing light dependent process which has a half-time of about 300 ms to reduce photoactivation yield by 50%. Figure 3B shows that maximum Y_{ss} occurs when the light pulses are separated by a dark interval of about 2−3 s, i.e. at a ratio $t_{dark}/t_{light} = 55-70$. These results are in agreement with earlier conclusions about sequential light−dark−light dependent steps in photoactivation [see reviews by Radmer and Cheniae (1977), Tamura and Cheniae (1987a,b), Ananyev et al. (1988b), and Miyao and Inoue (1991)].

Figure 3C shows that the half-time for photoactivation accelerates by about 4-fold from 250 to 60 s, while Y_{ss} increases by about 3-fold when the duration of the light pulse is increased from $t_{light} = 10$ to 180 ms. This suggests that the descending part of Figure 3A above 60 ms t_{light} can most likely be explained by increased photoinhibition of the reaction center photochemistry.

Effect of the Redox Potential of the Medium. We have used ferricyanide as the electron acceptor for PSII because of the following advantages. (a) It is possible to use concentrations (0.8−1.2 mM K_3FeCN_6) that have sufficient redox capacity for complete photoactivation. (b) Neither ferricyanide nor the ferrocyanide reduction product interacts with the intact WOC, nor do they interfere with the kinetics of photoactivation.

Figure 4A shows the ferricyanide concentration dependence of the maximum photoactivation yield. Below 100 μM K_3FeCN_6, a rapid decrease in photoactivation yield occurs simply because an electron acceptor is required. Y_{ss} remains flat in the region between 0.1 and 0.6 mM K_3FeCN_6 and decreases slightly by 10−15% from 0.6 to 1.2 mM K_3FeCN_6. Ferricyanide concentrations of 0.8 mM were routinely used for the majority of our experiments.

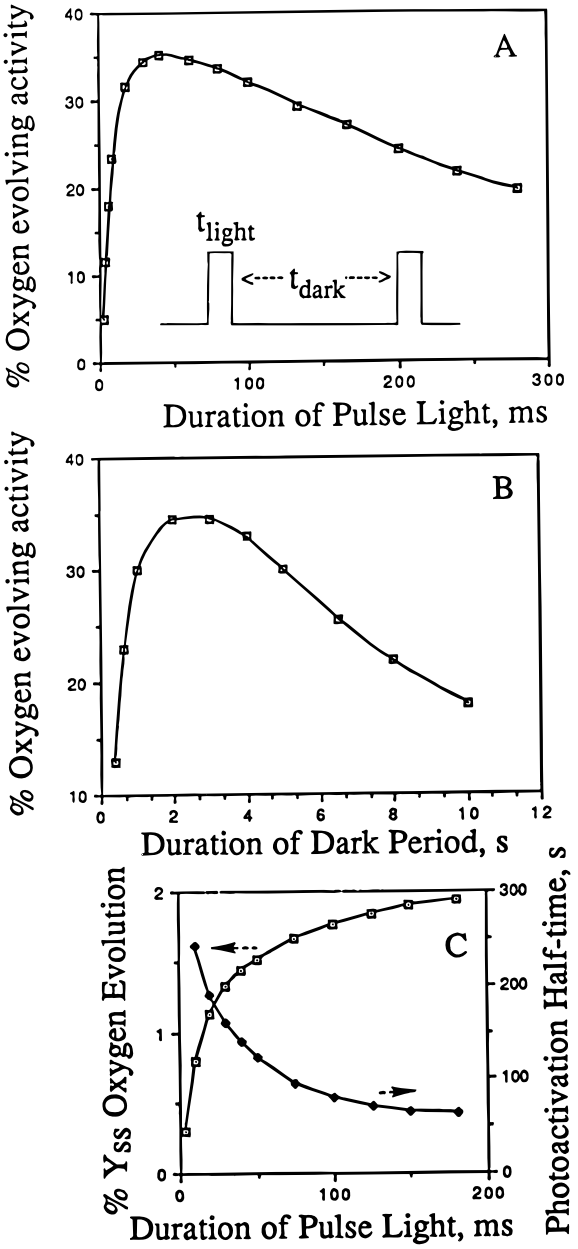

FIGURE 3: Dependence of the maximal rate of O_2 evolution (initial V_{O2}, examined under saturated continuous light illumination for 60 s) following photoactivation by pulse light illumination using (A) variable duration light pulses t_{light} at fixed t_{dark} = 2 s, (B) variable duration dark period t_{dark} at fixed t_{light} = 40 ms, and (C) dependence on t_{light} (at fixed t_{dark} = 2 s) of the maximum steady-state level of O_2 evolution recovered by photoactivation (Y_{ss}) and the half-time of photoactivation ($t_{1/2}$). The insert illustrates the pulse light profile. The measurement conditions were as follows: assay medium (pH 6.0), 8 μM $MnCl_2$, 10 mM $CaCl_2$, 1.2 mM K_3FeCN_6, 250 μg of Chl per mL, and I_p = 80 mW/cm^2. For other experimental details, see Materials and Methods.

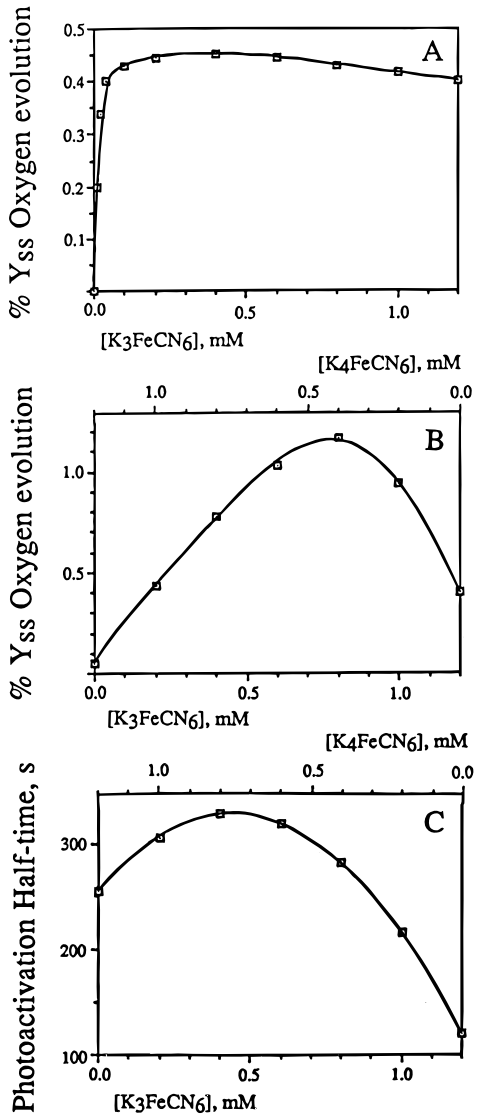

FIGURE 4: Dependence of the yield, Y_{ss}, and the half-time, $t_{1/2}$, for photoactivation on the redox potential of the medium. The maximum of yield Y_{ss} (A) in the presence of different concentrations of K_3FeCN_6 only and (B) in the presence of a mixture of K_3FeCN_6 + K_4FeCN_6. (C) The dependence of the half-time on the ratio K_3FeCN_6/K_4FeCN_6. The total concentration of K_3FeCN_6 + K_4FeCN_6 is constant at 1.2 mM in panels B and C.The assay conditions are the same as those in Figure 1.

In Figure 4B, the redox potential was adjusted using a variable ratio of K_3FeCN_6/K_4FeCN_6 at a fixed total concentration of 1.2 mM. A maximum in Y_{ss} activity is observed when the medium reduction potential (E_m) equals = 380 mV. The ascending portion of the titration of Y_{ss} has E_m = 330 mV, while the descending portion of the curve has E_m = 440 mV.

In Figure 4C, the half-time for recovery of photoactivation is seen to slow from 120 to 330 s when the ratio K_3FeCN_6/K_4FeCN_6 is decreased from 1.2/0 to 0.4/0.8, respectively. The half-time is 330 s at the maximum of the midpoint reduction potential curve where the E_m = 340 mV.

Figure 5a−c shows that the kinetics of photoactivation using 50 μM DCIP as the electron acceptor instead of ferricyanide are the same as with 50 μM K_3FeCN_6, while 50 μM DCBQ, an effective acceptor in intact PSII membranes, completely abolishes photoactivation. The latter behavior has been noted before and attributed to deactivation of intermediates of the Mn-tetrameric cluster by diffusible semi- and dihydroquinone products (Klimov et al., 1987; Miyao & Inoue, 1991).

The data in Figure 5d−f clearly indicate that addition of 50 μM DCIP or DCBQ as mediators of electron transport together with 0.8 mM K_3FeCN_6 did not change the biphasic kinetics of photoactivation but did increase Y_{ss}. The same increase in Y_{ss} is observed if DCBQ is added after photoactivation is completed with ferricyanide alone and is greater if steady-state V_{O2} is measured. This behavior indicates that DCBQ is simply acting as a faster electron acceptor than

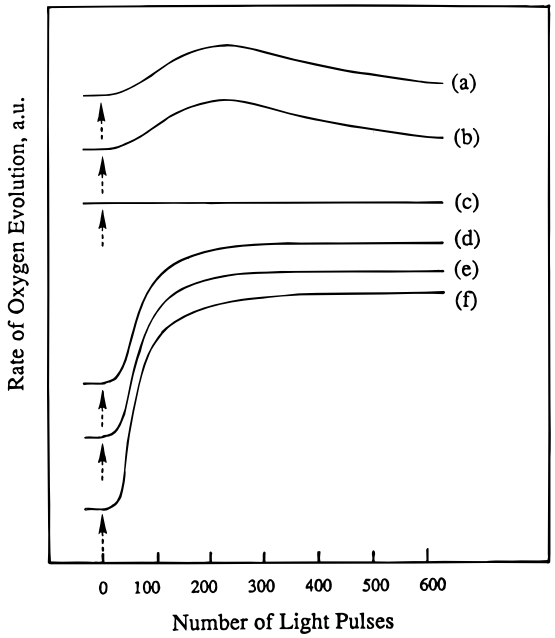

FIGURE 5: Effect of electron acceptors on the time course kinetics of photoactivation: (a) 50 μM DCIP, (b) 50 μM K_3FeCN_6, (c) 50 μM DCBQ, (d) 0.8 mM K_3FeCN_6, (e) a mixture of 50 μM DCIP + 0.8 mM K_3FeCN_6, (f) a mixture of 50 μM DCBQ + 0.8 mM K_3FeCN_6. The assay contained 8 μM Mn^{2+}, 10 mM $CaCl_2$, and 250 μg of Chl per mL.The conditions of pulse light illumination are as follows: t_{light} = 30 ms, t_{dark} = 2 s.

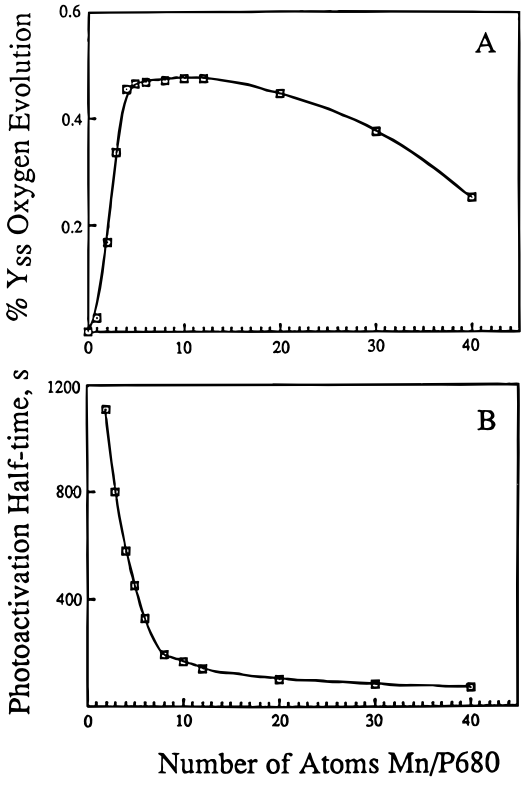

FIGURE 6: Dependence of the yield, Y_{ss}, (A), and the half-time, $t_{1/2}$ (B) for photoactivation in TPDBA-extracted PSII membrane fragments on the concentration of added $MnCl_2$. The conditions for pulse light photoactivation are the same as those in Figure 1. For other experimental details, see Materials and Methods.

ferricyanide but does not increase the fraction of photoactivated centers of WOC.

Four Mn^{2+} Ions/PSII Are Required for Photoactivation. Using TPDBA-extracted PSII membranes, we find that better than 95% of the Y_{ss} O_2 evolution could be recovered with 4.0 Mn/P680 (Figure 6A). From the monophasic rising portion of the titration curve, where the four Mn ions are taken up, a single Michaelis constant for photoactivation is evident with K_M = 2.6 μM Mn^{2+}. When only 2.0 Mn/P680 are present, Y_{ss} decreases to 38% of that observed with 4.0 Mn, while 3.0 Mn gives 74% of this rate. These data suggest that each active WOC requires exactly 4 Mn for maximal activity and that Mn uptake prior to attainment of the active cluster is reversible and cooperative, such that partially formed inactive clusters can disassemble and redistribute Mn to form active tetranuclear clusters. The rate-limiting step in photoactivation under these conditions involves a step which follows the binding of 4.0 Mn/P680. Figure 6A also reveals that Y_{ss} remains constant between 4 and 12 Mn/P680 and decreases above this concentration, with 50% loss occurring near 40 Mn/P680.

Figure 6B reveals that addition of 2−40 Mn/P680 accelerates the half-time for photoactivation from $t_{1/2}$ = 1200 to 80 s, with two phases evident at intermediate concentrations: a high-affinity subset (<5 Mn/P680) (Girardi & Seibert, 1992), having the strongest differential influence on acceleration of photoactivation, and a low-affinity subset, having at least a 100-fold weaker influence (shallower slope) on the rate of photoactivation. Analysis of the data suggests two curves with exponential dependences on Mn concentration: an initial acceleration from 1 to 5 Mn/P680 and a second phase from 8 to 40 Mn/P680. The initial slope of $t_{1/2}$ on Mn concentration can be analyzed as a power law dependence in $[Mn]^n$ with n = 1.1−1.2 as the Mn concentration approaches zero. These data indicate that the rate-limiting step in photoactivation (Figure 2, slope 2) requires uptake of 1 Mn/RC.

From Figure 6A,B, we can conclude that exactly 4 atoms of Mn are required for maximal recovery of O_2 evolution, while additional Mn^{2+} ions accelerate the rate of recovery of O_2 evolution but decrease the yield above 12 Mn/P680. These two Mn concentration dependencies suggest two distinct functions or different sites, or alternatively, this may reflect sample heterogeneity. Note also that the 50% loss of Y_{ss} evident in Figure 6A from 12 to 40 Mn atoms is not associated with any kinetic limitations on assembly of the active clusters and thus could reflect Mn^{2+} inhibition of fully assembled active clusters or, alternatively, inhibition of electron transport at another site. The apparent inhibition constant for Mn^{2+} at this site is ~40 μM.

DISCUSSION

Four Mn Are Required for Photoactivation. The complete removal of all Mn from the PSII membranes proved to be an essential requirement for observation of both reliable Mn binding stoichiometry (Figure 6) and the resolution of the new kinetic phase (Figure 2). Manganese extraction by chelation with TPDBA proved to be the most reliable method for this purpose. A comparison of several chelators for extraction of the inorganic cofactors and for photoactivation will be the subject of a separate paper.

The new microcell, at a standard concentration of 250 μg of Chl/mL, permits detection of less than 1/250 molecules of O_2 per single turnover flash at a S/N ratio of 5/1, enabling detection of O_2 at ~5 × 10^{-14} mol or ~3 × 10^{10} molecules of O_2 per flash seen in the photoactivated sample. The use

of an AC-coupled amplifier capable of both low- and high-frequency filtering between 0.3 and 3 Hz allows discrimination between rapid flash artifacts which exceed the response time of the electrode and slower base line changes which arise from O_2 uptake. The latter signal is small and can be seen using continuous illumination (Figure 1B, lines b′ and c′), while it is absent using pulse light excitation and filtering (Figure 1A, lines b and c).

Using this improvement in sensitivity, the titration experiment in Figure 6 demonstrates that precisely 4.0 Mn^{2+} ions are required for maximal recovery of photoactivation. These data offer a direct and accurate link between Mn stoichiometry and water oxidation, compared to Mn stoichiometry based on the number of Mn atoms bound to or released from PSII membranes (Callahan & Cheniae, 1985; Sivaraja & Dismukes, 1988; Sivaraja et al., 1988; Cheniae & Martin, 1971, 1972; Pauly & Witt, 1992).

Moreover, on the basis of the observation in Figure 6A showing a single Michaelis constant for the steady-state photoactivation process ($K_M = 2.6$ μM Mn^{2+}), we conclude that the assembly process allows rapid exchange (compared to $t_{1/2}$) between partially assembled clusters and cooperative uptake of the 4 Mn^{2+} ions. This behavior supports a model in which binding and photooxidation of each Mn^{2+} ion leads to formation of a higher-affinity site for the next Mn^{2+} ion. Such a model predicts that new ligands are formed either by protein conformational changes or by coupled proton ionization to yield μ-hydroxide or μ-oxo ligands (eq I):

$$\text{apo-PSII}(Mn^{2+}) \xrightarrow[FeCN^{+}]{h\nu} \text{apo-PSII}(Mn^{3+}) \xrightarrow[\text{H-OH}]{h\nu} \text{apo-PSII}(Mn^{3+})-OH \quad \text{(I)}$$

A New Kinetic Intermediate. Earlier studies have predicted the existence of sequential Mn dependent photooxidation steps separated by a dark step, on the basis of flash experiments like those in Figure 3 (Tamura & Cheniae, 1987a,b; Ananyev et al., 1988b). The data in Figure 2 reveal the first direct kinetic evidence for an intermediate prior to the steady-state rate-limiting step in photoactivation. The inability to detect the initial pre-steady-state intermediate in the earlier studies appears to be due to either or all of the following factors: the lack of complete Mn extraction, the need to use much higher Mn concentrations for maximal photoactivation (~1000 μM Mn^{2+}), and the presence of residual hydroxylamine or Tris free base used for prereduction and extraction of Mn from the WOC (Cheniae & Martin, 1978; Miller & Brudvig, 1989; Tamura & Cheniae, 1987a,b; Blubaugh & Cheniae, 1990).

The disappearance of the initial kinetic phase with increasing Mn concentration in the medium (Figure 2) is strong evidence supporting a model in which there are two kinetic phases in sequence for all PSII centers, rather than two populations of centers with different rates of photoactivation. This behavior was seen with all samples for which Mn is completely removed. The slower rate of the initial phase compared to the second phase indicates that it involves formation of a pre-steady-state intermediate and not the rate-limiting step under steady-state conditions. A detailed study of the break point, the initial slope, and the steady-state slope on Mn^{2+} and Ca^{2+} concentrations will be examined in a forthcoming study.

Effects of the Light−Dark Pulse Duration on Photoactivation Yield. The effects of repetitive single (Radmer & Cheniae, 1971; Tamura & Cheniae, 1987a,b; Miyao & Inoue, 1991) and repetitive double (Ananyev et al., 1988b) xenon flashes at variable intervals on the yield of photoactivation were reported previously. Our data (Figure 3A,B) confirm the requirements for sequential light−dark−light steps during photoactivation.

A possible explanation for the rise time of 8−10 ms seen in Figure 3A could be that there is an insufficient number of photons to ensure saturation of all PSII centers, since double flash experiments with a xenon lamp showed a rise time of 250 μs (Ananyev et al., 1988b). This conclusion is in agreement with the time ($\tau \sim 250$ μs) of uniform turnover of PSII (Kok et al., 1970; Zankel, 1973). The descending phase of $t_{1/2} > 300$ ms in Figure 3A has been previously attributed to photoinhibition that occurs in the absence of an electron donor in Mn-depleted PSII membranes (Klimov et al., 1990a,b; Blubaugh & Cheniae, 1990).

The optimal dark period between single repetitive flashes is absolutely essential for photoactivation (Tamura & Cheniae, 1987a,b; Klimov et al., 1987; Ananyev et al., 1988a,b; Miyao & Inoue, 1991). Our experiments made with TPDBA-treated PSII membranes in the presence of 8 μM Mn^{2+}, 8 mM $CaCl_2$, and 0.8 mM K_3FeCN_6 show that a dark period shorter than $t_{1/2} \sim 0.5$ s and longer than $t_{1/2} \sim 6$ s leads to decreases in Y_{ss}. Thus, an unstable intermediate is produced which has a half-life approximately 4−6 times longer than that found in NH_2OH-treated PSII membranes in the presence of 100 μM DCIP (Tamura & Cheniae, 1987a,b).

Redox Potential of Medium. In the present study, we have found that the yield and rate of photoactivation show a strong dependence on the reduction potential of the medium using the ferri-/ferrocyanide couple. As shown in Figure 4B,C, an increase in the ratio of K_3FeCN_6 to K_4FeCN_6 markedly increased Y_{ss} and delayed $t_{1/2}$ with break points at a ratio of 2/1 and 1/2, respectively. However, the initial lag-phase (slope 1 in Figure 2) is independent of the electron acceptors used (Figure 5). Thus, in contrast to electron donors such as H_2O_2, DPC, NH_2OH, NH_2NH_2, and $DCIPH_2$ (Miyao & Inoue, 1991; Blubaugh & Cheniae, 1992), ferrocyanide ($C < 0.5$ mM) does not disrupt the process of photoactivation. We suggest that the effect of reduction potential of the medium is due to (1) elimination of charge recombination between Y_z^+ and electron acceptors or donors, possibly cytochrome b_{559} [see the effect of K_4FeCN_6 on photoinducible signal II (Babcock & Sauer, 1975; Yuasa et al., 1983)]; (2) stabilization of intermediate(s) in the assembly process by elimination of contamination by nonfunctional Mn^{3+} surrounding the active site of the WOC (Chen et al., 1995); and (3) elimination of photoinhibition by protection of apo-PSII against photobleaching of carotenoids (Klimov et al., 1990a,b).

ACKNOWLEDGMENT

We are grateful to Dr. P. J. Pessiki for synthesis of the Mn−Ca−chelator TPDBA and L. Zaltsman for her help in preparation of the article. Professors G. W. Brudvig, G. M. Cheniae, V. V. Klimov, and A. W. Rutherford have provided useful advice.

REFERENCES

Ananyev, G. M., Shafiev, M. A., & Klimov, V. V. (1988a) *Biofizika 4*, 594−599.

Ananyev, G. M., Shafiev, M. A., Isaenko, T. V., & Klimov, V. V. (1988b) *Biofizika 33*, 285−289.

Ananyev, G. M., Wydrzynski, T., Renger, G., & Klimov, V. V. (1992) *Biochim. Biophys. Acta 1100*, 303−311.

Babcock, G. T., & Sauer, K. (1975) *Biochim. Biophys. Acta 376*, 315−328.

Berthold, D. A., Babcock, G. T., & Yocum, C. F. (1981) *FEBS Lett. 134*, 231−234.

Blubaugh, D. J., & Cheniae, G. M. (1990) *Biochemistry 29*, 5109−5118.

Blubaugh, D. J., & Cheniae, G. M. (1992) in *Research in Photosynthesis* (Murata, N., Ed.) Vol. II, pp 361−364, Kluwer Academic Publishers, Dordrecht, The Netherlands.

Brudvig, G. W., Beck, W. F., & De Paula, J. C. (1989) *Annu. Rev. Biophys. Chem. 18*, 25−46.

Callahan, F. E., & Cheniae, G. M. (1985) *Plant Physiol. 79*, 777−786.

Chen, C., Kazimir, J., & Cheniae, G. M. (1995) *Biochemistry 34*, 13511−13526.

Chen, G.-X., Kazimir, J., & Cheniae, G. M. (1992) *Biochemistry 31*, 11072−11083.

Cheniae, G. M. (1980) *Methods Enzymol. 69*, 349−363.

Cheniae, G. M., & Martin, I. F. (1971) *Biochim. Biophys. Acta 253*, 167−181.

Cheniae, G. M., & Martin, I. F. (1972) *Plant Physiol. 50*, 87−94.

Cheniae, G. M., & Martin, I. F. (1978) *Biochim. Biophys. Acta 502*, 321−344.

Debus, R. J. (1992) *Biochim. Biophys. Acta 1102*, 269−353.

Dismukes, G. C. (1986) *Photochem. Photobiol. 43*, 99−115.

Dismukes, G. C., Ferris, K., & Watnick, P. (1982) *Photobiochem. Photobiophys. 3*, 243−256.

Ebina, M., & Yamashita,T. (1992) in *Research in Photosynthesis* (Murata, N., Ed.) Vol. II, pp 389−392, Kluwer Academic Publishers, Dordrecht, The Netherlands.

Ghanotakis, D. F., Babcock, G. T., & Yocum, C. F. (1984) *Biochim. Biophys. Acta 765*, 388−398.

Girardi, M. L., & Seibert, M. (1992) in *Research in Photosynthesis* (Murata, N., Ed.) Vol. II, pp 357−560, Kluwer Academic Publishers, Dordrecht, The Netherlands.

Horowitz, P., & Hill, W. (1993) *The Art of Electronics*, Cambridge University Press, Cambrige, London, New York, New Rochelle, Melbourne, and Sydney.

Hsu, B.-D., Lee, J.-Y., & Pan, R.-L. (1987) *Biochim. Biophys. Acta 890*, 89−96.

Klimov, V. V., Allakhverdiev, S. I., Shuvalov, V. A., & Krasnovsky, A. A. (1982) *Dokl. Akad. Nauk SSSR 263*, 1001−1007.

Klimov, V. V., Ganago, I. B., Allakhverdiev, S. I., Shafiev, M. A., & Ananyev, G. M. (1986) in *VII International Congress on Photosynthesis*, pp 304−393, August 10−15, Brown University, Providence, RI.

Klimov, V. V., Ganago, I. B., Allakhverdiev, S. I., Shafiev, M. A., & Ananyev, G. M. (1987) in *Progress in Photosynthesis Research* (Biggins, J., Ed.) Vol. 1, pp 581−584, Martinus Nijhoff Publishers, The Netherlands.

Klimov, V. V., Shafiev, M. A., & Allakhverdiev, S. I. (1990a) *Photosynth. Res. 23*, 59−65.

Klimov, V. V., Ananyev, G. M., Allakhverdiev, S. I., Zharmukhamedov, S. K., Mulay, M., Hegde, U., & Padhye, S. (1990b) in *Current Research in Photosynthesis* (Baltscheffsky, M., Ed.) Vol. I, pp 247−254, Kluwer Academic Publishers, Dordrecht, The Netherlands.

Kok, B., Forbush, B., & McGloin, M. (1970) *Photochem. Photobiol. 11*, 457−475.

Miller, A. F., & Brudvig, G. W. (1989) *Biochemistry 28*, 8181−8190.

Miller, A. F., & Brudvig, G. W. (1990) *Biochemistry 29*, 1385−1392.

Miyao, M., & Inoue, Y. (1991) *Biochim. Biophys. Acta 1056*, 47−56.

Miyao-Tokutomi, M., Ono, T.-A., & Inoue, Y. (1990) in *Current Research in Photosynthesis* (Baltscheffsky, M., Ed.) Vol. I, pp 909−912, Kluwer Academic Publishers, Dordrecht, The Netherlands.

Ono, T.-A., & Inoue, Y. (1983a) *Biochim. Biophys. Acta 723*, 191−201.

Ono, T.-A., & Inoue, Y. (1983b) in *The Oxygen Evolving System of Photosynthesis* (Inoue, Y., et al., Eds.) pp 337−344, Academic Press Japan, Tokyo, Japan.

Pauly, S., & Witt, H. T. (1992) *Biochim. Biophys. Acta 1099*, 211−218.

Preston, C., & Seibert, M. (1989) *Photosynth. Res. 22*, 101−103.

Preston, C., & Seibert, M. (1991) *Biochemistry 30*, 9615−9624.

Radmer, R., & Cheniae, G. M. (1971) *Biochim. Biophys. Acta 253*, 182−186.

Radmer, R., & Cheniae, G. M. (1977) in *Primary Process of Photosynthesis* (Barber, J., Ed.) pp 303−348, Elsevier, North-Holland Biomedical Press.

Shafiev, M. A., Ananyev, G. M., Allakhverdiev, S. I., Smolova, T. N., & Klimov, V. V. (1988) *Biofizika 33*, 61−65.

Sivaraja, M., & Dismukes, G. C. (1988) *Biochemistry 27*, 3467−3475.

Sivaraja, M., Hunziker, D., & Dismukes, G. C. (1988) *Biochim. Biophys. Acta 936*, 228−235.

Tamura, N., & Cheniae, G. M. (1987a) in *Progress in Photosynthesis Research*, Vol. I, pp 621−624, Martinus Nijhoff Publishers, The Netherlands.

Tamura, N., & Cheniae, G. M. (1987b) *Biochim. Biophys. Acta 890*, 179−194.

Tamura, N., Ikeuchi, M., & Inoue, Y. (1989a) *Biochim. Biophys. Acta 973*, 281−289.

Tamura, N., Inoue Y., & Cheniae, G. M. (1989b) *Biochim. Biophys. Acta 976*, 173−181.

Tamura, N., Kamachi, H., Hokari, N., Masumoto, H., & Inoue, H. (1991) *Biochim. Biophys. Acta 1060*, 51−58.

Tamura, N., Tanaka, T., Wakamatsu, K., Inoue, H., & Wada, K. (1992) in *Research in Photosynthesis* (Murata, N., Ed.) Vol. II, pp 405−408, Kluwer Academic Publishers, Dordrecht, The Netherlands.

Yamashita, T., & Tomita, G. (1974) *Plant Cell Physiol. 15*, 69−82.

Yamashita, T., & Ashizawa, A. (1983) in *The Oxygen Evolving System of Photosynthesis* (Inoue, Y., et al., Eds.) pp 327−336, Academic Press Japan, Tokyo, Japan.

Yuasa, M., Koike, H., & Inoue, Y. (1983) in *The Oxygen Evolving System of Photosynthesis* (Inoue, Y., et al., Eds.) pp 103−112, Academic Press Japan, Tokyo, Japan.

Zankel, K. (1973) *Biochim. Biophys. Acta 325*, 138−148.

BI952667H